



## 저작자표시 2.0 대한민국

이용자는 아래의 조건을 따르는 경우에 한하여 자유롭게

- 이 저작물을 복제, 배포, 전송, 전시, 공연 및 방송할 수 있습니다.
- 이차적 저작물을 작성할 수 있습니다.
- 이 저작물을 영리 목적으로 이용할 수 있습니다.

다음과 같은 조건을 따라야 합니다:



저작자표시. 귀하는 원저작자를 표시하여야 합니다.

- 귀하는, 이 저작물의 재이용이나 배포의 경우, 이 저작물에 적용된 이용허락조건을 명확하게 나타내어야 합니다.
- 저작권자로부터 별도의 허가를 받으면 이러한 조건들은 적용되지 않습니다.

저작권법에 따른 이용자의 권리는 위의 내용에 의하여 영향을 받지 않습니다.

이것은 [이용허락규약\(Legal Code\)](#)을 이해하기 쉽게 요약한 것입니다.

[Disclaimer](#) 

2015년 2월

석사학위 논문

# Hydrogen Evolution Catalyzed by ( $\eta^6$ -arene)Cr(CO)<sub>3</sub>: Observation of $\sigma$ -borane complexes in solution

조선대학교 대학원

화 학 과

이 혜 선

( $\eta^6$ -arene)Cr(CO)<sub>3</sub> 에 의해  
촉매화된 수소방출 : 용액안에서의  
 $\sigma$ -borane 관찰

Hydrogen Evolution Catalyzed by ( $\eta^6$ -arene)Cr(CO)<sub>3</sub>:  
Observation of  $\sigma$ -borane complexes in solution

2015년 2월 25일

조 선 대 학 교 대 학 원

화 학 과

이 혜 선

( $\eta^6$ -arene)Cr(CO)<sub>3</sub> 에 의해  
촉매화된 수소방출 : 용액안에서의  
 $\sigma$ -borane 관찰

지도교수 이 종 대

이 논문을 이학석사학위신청 논문으로 제출함.

2014년 10월

조 선 대 학 교 대 학 원

화 학 과

이 혜 선

## 이혜선의 석사학위논문을 인준함

위원장    조선대학교    교수    류    설    (인)

위    원    조선대학교    교수    김    호    중    (인)

위    원    조선대학교    교수    이    종    대    (인)

2014년 11월

조 선 대 학 교 대 학 원

# TABLE OF CONTENTS

TABLE OF CONTENTS	1
LIST OF FIGURES	3
LIST OF TABLE	4
ABSTRACT	

## Hydrogen Evolution Catalyzed by ( $\eta^6$ -arene)Cr(CO)<sub>3</sub>: Observation of $\sigma$ -borane complexes in solution

1.	<b>Abstract.....</b>	5
2.	<b>Introduction.....</b>	7
3.	<b>Experimental.....</b>	8
3.1.	General consideration.....	8
3.2.	Crystal Structure Determination.....	9
3.3.	Density Functional Calculations.....	10
3.4.	Synthesis of 1-(phenyl- $\eta^6$ -chromium(0) tricarbonyl) -2-phenyl-o-carborane (3a).....	10

3.5.	Synthesis of 1,2-bis(phenyl- $\eta^6$ -chromium(0)tricarbonyl)-o-carborane (3b).....	11
3.6.	Catalytic dehydrogenation of ammonia-borane ( $\text{H}_3\text{N-BH}_3$ , AB) under photolytic condition.....	11
3.7.	Photolysis of ( $\eta^6\text{-C}_6\text{H}_6$ )Cr(CO) <sub>3</sub> in presence of tertbutyl tertbutylamine-borane ( $\text{tBuH}_2\text{N-BH}_3$ , TBAB).....	13
3.8.	Photolysis of ( $\eta^6\text{-arene}$ )Cr(CO) <sub>3</sub> in presence of trimethyl amine-borane ( $\text{Me}_3\text{N-BH}_3$ , TMAB).....	13
3.9.	Characterization of $\sigma$ -borane complexes.....	13
4.	Results and Discussion.....	14
5.	Conclusion.....	28
6.	References.....	29

## LIST OF FIGURES

---

- Figure 1** ORTEP drawing (30% probability for thermal ellipsoids) of 3a
- Figure 2** ORTEP drawing (30% probability for thermal ellipsoids) of 3b (the hydrogen atoms are omitted for clarity).
- Figure 3** H<sub>2</sub> evolution profile of the reaction between 3b and ammonia-borane.
- Figure 4** Energy levels and isodensity plots (isodensity contour = 0.03 a.u.) for selected occupied and unoccupied molecular orbitals of 3a obtained by DFT calculations.
- Figure 5** Energy levels and isodensity plots (isodensity contour = 0.03 a.u.) for selected occupied and unoccupied molecular orbitals of 3b obtained by DFT calculations.
- Figure 6** AB dehydrogenation kinetic profiles for ( $\eta^6$ -arene)Cr(CO)<sub>3</sub> catalysts 1, 2, 3a, and 3b.
- Figure 7** (a) Dehydrogenation kinetic isotope effect (KIE) plots for AB and deuterated ABs with catalyst 3b at 25 °C and (b) their corresponding logarithmic plots. The straight lines in (b) were obtained from linear regression analysis of the data points.
- Figure 8**
- Figure 9**
- Figure 10**
- Figure 11**



## LIST OF TABLES

---

Table 1	Crystal data and structure refinement
Table 2	Selected bond lengths [ $\text{\AA}$ ] and torsion angles [ $^{\circ}$ ] for <b>3a</b> and <b>3b</b>
Table 3	
Table 4	
Table 5	

## Abstract

### Hydrogen Evolution Catalyzed by ( $\eta^6$ -arene)Cr(CO)<sub>3</sub>: Observation of $\sigma$ -borane complexes in solution

Lee Hye Sun

Advisor : Prof. Lee Jong Dae, Ph.D,

Department of Chemistry,

Graduate School of Chosun University

arene chromium tricarbonyl complexes 에서 chromium(0) 중심과 접한 amine-boranes의 B-H 시그마 결합의 활성이 연구되고 있다. ammonia-borane 과 tert-butylamine-borane 의 존재 하에 있는 크롬아렌화합물의 광분해를 하면 수소방출과 BNH<sub>x</sub> 폴리머의 침전이 일어난다. 달리 말하면, trimethylamine-borane 존재 하에 있는 광분해로  $\sigma$ -borane 혼합물의 형성이 일어난다.  $\sigma$ -borane화합물 ( $\eta^6$ -arene)Cr(CO)<sub>2</sub>( $\eta^1$ -HBH<sub>2</sub>-NMe<sub>3</sub>) (arene = fluorobenzene 4, benzene 5, and diphenyl-o-carborane 6)는 <sup>1</sup>H, <sup>11</sup>B, and <sup>13</sup>C NMR 분광학에 의해 용액에서 특징지어진다. 전자를 끄는 치환기가 있는 벤젠고리는 이러한 종류의 화합물에 있는  $\sigma$ -borane 일부분을 더 안정하게 해준다.

## 1. Introduction

In the area of organometallic chemistry  $\sigma$ -borane complexes became useful species demonstrating their significance in catalysis, hydrogen storage, and synthesis of polymers of main group elements, etc. The most interesting feature of these complexes is a naked sigma bond acting as a ligand revealing an unusual binding mode in coordination chemistry. Besides, these complexes are described as models and thus isolable analogs of  $\sigma$ -alkane complexes which are only observed transiently at low temperatures. Although  $\sigma$ -borane complexes came into focus with metal-dihydrogen sigma complexes contemporarily, its impact on organometallic chemistry and consequences are being disclosed very recently. The difficulties involved in the synthesis and in certain cases not isolable, of these rather unstable species have hampered progress of this interesting class of compounds. Despite the difficulties, the typical  $\eta^2$ -binding mode of tri-coordinated boranes to the metal center, where back donation of filled metal d-orbital to empty p-orbitals of borane stabilizes a complicated 4-centered-4-electron bond has been established. Shimoi and co-workers synthesized and structurally characterized  $\sigma$ -borane complexes, in which a tetra-coordinated boron is coordinated to the metal in an  $\eta^1$ -fashion. In this type of binding mode,  $\sigma^*$  orbitals of boranes of high energy rule out any back donation. The  $\sigma$ -borane complexes reported to date have all had  $\eta^5$ -C<sub>5</sub>H<sub>5</sub> co-ligand. As yet there are no examples of  $\sigma$ -borane complexes bearing  $\eta^6$ -arene co-ligand.

Photolysis of ( $\eta^6$ -arene)Cr(CO)<sub>3</sub> results in a coordinatively unsaturated, 16 electron species ( $\eta^6$ -arene)Cr(CO)<sub>2</sub>. Recently, Heinekey and co-workers noted the formation of sigma dihydrogen complexes in the reaction of substituted arene chromium tricarbonyl complex with H<sub>2</sub> under photolytic conditions using NMR spectroscopy. However,

attempts to isolate the dihydrogen complex afforded the oxidative addition product. Reaction of silanes with  $(\eta^6\text{-arene})\text{Cr}(\text{CO})_3$  complexes under photolytic conditions has also been studied. The binding and activation of the relatively strong H-X (X = H, Si, B)  $\sigma$ -bonds in small molecules are subjects of active current research interest and they serve as models for the binding and activation of the strong C-H  $\sigma$ -bond in methane and other higher alkanes. We chose the photolysis of  $(\eta^6\text{-arene})\text{Cr}(\text{CO})_3$  in presence of amine-borane adducts to explore this area expecting a  $\sigma$ -borane complex and activation of B-H  $\sigma$ -bond on Cr(0) center which possesses an arene ligand.

With a view to obtain relatively stable  $\sigma$ -borane complexes of chromium bearing arene and CO ligands, we carried out the photolysis of  $(\eta^6\text{-arene})\text{Cr}(\text{CO})_3$  in the presence of amine-boranes. We attempted to change the substituent on arene so as to realize a system with the right electronic features to enable to obtain a stable  $\sigma$ -borane complex. Herein, we report the synthesis and spectroscopic characterization of  $\sigma$ -borane complexes of chromium bearing arene and carbonyl ligands.

## 2. Experimentals

### General considerations.

All manipulations were performed under dry argon or nitrogen atmosphere using standard Schlenk line techniques. Tetrahydrofuran, toluene, benzene, n-hexane, and mesitylene were dried thoroughly over sodium benzophenone whereas  $\text{P}_2\text{O}_5$  was used for drying fluorobenzene and dichloromethane and distilled prior to use.  $\text{Cr}(\text{CO})_6$  and the substituted amine-boranes were purchased from Aldrich.  $\text{Cr}(\text{CO})_6$  was purified by sublimation before use. Ammonia-borane ( $\text{H}_3\text{N-BH}_3$ , AB)<sup>19</sup>,  $(\eta^6\text{-C}_6\text{H}_5\text{F})\text{Cr}(\text{CO})_3$ ,  $(\eta^6\text{-C}_6\text{H}_6)\text{Cr}(\text{CO})_3$ ,<sup>20</sup>  $(\eta^6\text{-Ph}_2\text{-o-carborane})\text{Cr}(\text{CO})_3$ , and  $(\eta^6\text{-C}_6\text{H}_5\text{F})\text{Cr}(\text{CO})_3$  were used as received.

${}^6\text{-Ph}_2\text{-o-carborane)[Cr(CO)}_3]_2$ ,<sup>21</sup> were synthesized and characterized following literature procedures. The arene chromium tricarbonyl complexes were recrystallized by slow diffusion of n-hexane to their concentrated dichloromethane solution and bright yellow or reddish-yellow colored crystals obtained were washed with n-hexane and dried under vacuum. Trimethylamine-borane ( $\text{Me}_3\text{N-BH}_3$ , TMAB) was purified by sublimation before use whereas tert-butylamine-borane ( ${}^t\text{BuH}_2\text{N-BH}_3$ , TBAB) was used as received. Photolysis of the NMR spectral samples immersed in low temperature slush bath were done using a 400 W high pressure mercury vapor lamp ( $\lambda = 400\text{ nm}$ ). The  ${}^1\text{H}$ ,  ${}^{13}\text{C}$  (75.4 MHz), and  ${}^{11}\text{B}$  (96.3 MHz) NMR spectral data were acquired using an Varian 300 MHz instrument. All  ${}^1\text{H}$  and  ${}^{13}\text{C}$  NMR spectral values reported herein are relative to the signals of the respective deuterated solvents used.  ${}^{11}\text{B}$  NMR spectral signals of the  $\sigma$ -borane complexes are reported with respect to the quartet signal of  $\text{Me}_3\text{N-BH}_3$  (TMAB) at -8.0 ppm ( $J_{\text{B-H}} = 97\text{ Hz}$ ). IR spectra of neat powder samples were obtained using a Bruker ALPHA-P spectrometer working in the 400-4500  $\text{cm}^{-1}$  range.

**Crystal Structure Determination.** Crystals of **3a** and **3b** were obtained from  $\text{CH}_2\text{Cl}_2$  /n-Hexane, sealed in glass capillaries under argon, and mounted on the diffractometer. Preliminary examination and data collection were performed using a Bruker SMART CCD detector system single-crystal X-ray diffractometer equipped with a sealed-tube X-ray source (40 kV  $\times$  50 mA) using graphite-monochromated Mo K $\alpha$  radiation ( $\lambda = 0.71073\text{ \AA}$ ). Preliminary unit cell constants were determined with a set of 45 narrow-frame ( $0.3^\circ$  in  $\varpi$  scans. The double-pass method of scanning was used to exclude any noise. The collected frames were integrated using an orientation matrix

determined from the narrow-frame scans. The SMART software package was used for data collection, and SAINT was used for frame integration. Final cell constants were determined by a global refinement of xyz centroids of reflections harvested from the entire data set. Structure solution and refinement were carried out using the SHELXTL-PLUS software package.

**Density Functional Calculations.** Full geometry optimizations of the complexes in their singlet ground state were performed with DFT using the B3LYP functional,<sup>24</sup> with the relativistic effective core potential and basis set tLanL2DZ<sup>25</sup> for the chromium and the 6-31G<sup>26</sup> basis set for the remaining atoms. No symmetry constraints were applied during the geometry optimizations, which were carried out with the Gaussian09 package.<sup>27</sup> The nature of the stationary points located was further checked by computations of harmonic vibrational frequencies at the same level of theory. All Isodensity plots (isodensity contour=0.03 a.u.) of the frontier orbitals were visualized by Chem3D Ultra program. The various properties of all compounds, such as HOMOs, LUMOs, and energy gaps were obtained from the computed results and were compared to the available experimental data. The excitation energies and oscillator strengths for the lowest 30 singlet-singlet transitions at the optimized geometry in the ground state were obtained in TDDFT calculations using the same basis set and functional as for the ground state. Frequency calculations of all carboranes including Raman data were calculated by the same functional basis set using an optimized structure. Simulated absorption spectra and Raman spectra of all carborane compounds were obtained by GaussSum 2.2 program.

**Synthesis of 1-(phenyl- $\eta^6$ -chromium(0) tricarbonyl)-2-phenyl-o-carborane (3a).** Diphenyl-o-carborane (0.37 g, 1.0 mmol) and  $[(\text{NH}_3)_3\text{Cr}(\text{CO})_3]$  (0.44 g, 2.0 mmol) were dissolved in a mixture of THF (5 mL) and di-*n*-butylether (50 mL). The mixture was

refluxed for 72h and the resulting dark reddish solution was cooled to room temperature and filtered over Celite. The solvents were evaporated under reduced pressure. After evaporation the crude reaction mixture was purified using column chromatography ( $\text{CH}_2\text{Cl}_2$ :Hexane eluent) to give chromium complex **3a**, and then recrystallized from hexane to obtain yellow crystals. Yield: 77% (0.35 g, 0.77 mmol). HRMS: Calcd for  $[\text{C}_{18}\text{H}_{25}\text{B}_{10}\text{CrO}_3]^+$  451.2139. Found: 451.2218. IR spectrum (KBr pellet,  $\text{cm}^{-1}$ ):  $\nu(\text{B}-\text{H})$  2583, 2589;  $\nu(\text{CO})$  1960, 1892.  $^1\text{H}$  NMR ( $\text{CDCl}_3$ , 300.1 MHz)  $\delta$  7.62 (m, 4H, Ph-*H*), 6.74 (d,  $J_{\text{C-H}} = 14$  Hz, 1H, Ph-*H*), 6.52 (t,  $J_{\text{C-H}} = 13$  Hz, 3H, Ph-*H*), 6.48 (d,  $J_{\text{C-H}} = 14$  Hz, 1H, Ph-*H*).  $^{13}\text{C}$  NMR ( $\text{CDCl}_3$ , 75.4 MHz)  $\delta$  230.4 (Cr-CO), 141.0, 134.9, 133.8, 133.7, 131.0, 128.8, 126.7 (Ph), 85.6 (Ph-Ccab).  $^{11}\text{B}$  NMR ( $\text{CDCl}_3$ , 96.3 MHz)  $\delta$  -3.11 (3B), -8.54 (3B), -8.71 (2B), -10.37 (1B), -14.84 (1B).

**Synthesis of 1,2-bis(phenyl-h6-chromium(0) tricarbonyl)-o-carborane (3b).** A procedure analogous to the preparation of **3a** was used and obtained a orange crystals. Yield: 64% (0.59 g, 0.64 mmol). HRMS: Calcd for  $[\text{C}_{22}\text{H}_{30}\text{B}_{10}\text{Cr}_2\text{O}_6]^+$  604.1783. Found: 604.2011. IR spectrum (KBr pellet,  $\text{cm}^{-1}$ ):  $\nu(\text{B}-\text{H})$  2580, 2591;  $\nu(\text{CO})$  1971, 1896.  $^1\text{H}$  NMR ( $\text{CDCl}_3$ , 300.1 MHz)  $\delta$  6.67 (d,  $J_{\text{C-H}} = 14$  Hz, 2H, Ph-*H*), 6.52 (t,  $J_{\text{C-H}} = 12$  Hz, 6H, Ph-*H*), 6.48 (d,  $J_{\text{C-H}} = 14$  Hz, 2H, Ph-*H*).  $^{13}\text{C}$  NMR ( $\text{CDCl}_3$ , 75.4 MHz)  $\delta$  232.1 (Cr-CO), 139.5, 136.9, 133.8, 131.7, 130.3, 129.8, 128.0 (Ph), 85.0 (Ph-Ccab).  $^{11}\text{B}$  NMR ( $\text{CDCl}_3$ , 96.3 MHz)  $\delta$  -4.11 (3B), -8.84 (3B), -9.51 (2B), -12.47 (1B), -15.88 (1B).

### Catalytic dehydrogenation of ammonia-borane ( $\text{H}_3\text{N}-\text{BH}_3$ , AB) under photolytic condition

The reactor consisted of modified 150 mL double jacket glassware. A three-way

connector was modified to allow the system to be purged with argon gas and to allow the hydrogen gas produced during the dehydrogenation reaction to pass through the mass flow meter (MFM). The apparatus enabled the catalyst to be injected into the reactor without exposing the reactants to air. The reaction temperature was monitored and controlled with a thermocouple and an external heater/cooler (chiller), respectively. The experimental procedure involved filling the reactor with 2 mL of a tetraglyme solution containing 1.46 mmol of AB. The reactor was subsequently flushed with argon for at least 30 min to minimize the moisture level inside the vessel. After thermal equilibration of the reactor and the low temperature trap, 3 mol% of catalysts **1**, **2**, **3a**, and **3b** were dissolved in 0.5 mL nitromethane (MeNO<sub>2</sub>) and injected into the AB solution. Reaction time began at the time when the catalyst was introduced into the mixture and ended when H<sub>2</sub> evolution ceased. The progress of the reaction was monitored by examining the amount of hydrogen generated using a volumetric technique that allowed real time tracking of the reaction.<sup>8</sup> MeNO<sub>2</sub> (bp. 101 °C) and other volatiles including NH<sub>3</sub> in the product stream were anticipated because of the large exothermy expected under the experimental conditions, even though the reactor temperature was controlled at 25 °C. In the apparatus, a -90 °C low temperature bath (liquid N<sub>2</sub> with CH<sub>2</sub>Cl<sub>2</sub>) trapped the volatiles to ensure that the gas volume measured as it passed through the MFM system was only due to hydrogen. After dehydrogenation, the solid remaining in the reactor was collected through filtration, rinsed with Et<sub>2</sub>O and dried *in vacuo*. Because of the fast hydrogen release kinetics for catalyst **3b**, there was the possibility of a heterogeneous pathway. That possibility was examined either by the supplemental



addition of AB after dehydrogenation or through mercury poisoning as previously described. The H<sub>2</sub> release kinetics was not altered following either of those actions.

**Photolysis of ( $\eta^6$ -C<sub>6</sub>H<sub>6</sub>)Cr(CO)<sub>3</sub> in presence of tertbutylamine-borane ( $t$ -BuH<sub>2</sub>N-BH<sub>3</sub>, TBAB)**

tert-Butylamine-borane (5.3 mg, 0.06 mmol) and ( $\eta^6$ -C<sub>6</sub>H<sub>6</sub>)Cr(CO)<sub>3</sub> (5 mg, 0.02 mmol) were dissolved in 0.5 mL of toluene in a NMR tube fitted with a septum. The NMR tube was placed in a quartz tube containing ice to maintain the temperature at 273 K. The entire setup was exposed to UV radiation and the NMR spectra were recorded at definite time intervals.

**Photolysis of ( $\eta^6$ -arene)Cr(CO)<sub>3</sub> in presence of trimethylamine-borane (Me<sub>3</sub>N-BH<sub>3</sub>, TMAB): formation of  $\sigma$ -borane complexes**

( $\eta^6$ -Arene)Cr(CO)<sub>3</sub> and Me<sub>3</sub>N-BH<sub>3</sub> were transferred into a Wilmad high pressure NMR tube inside the glove box. It was then charged with 0.5 mL of toluene-*d*<sub>8</sub>. The contents of the NMR tube were then degassed by freeze-pump-thaw technique. Then the tube was immersed in an acetone-liquid N<sub>2</sub> slush bath inside a quartz tube maintained at 213 K. The solution was irradiated for 1 h at this temperature. CO gas produced inside the NMR tube was removed by

freeze-pump-thaw technique after the reaction. Then the tube was inserted into a NMR probe pre-cooled to 213 K and the NMR data were acquired at different temperatures.

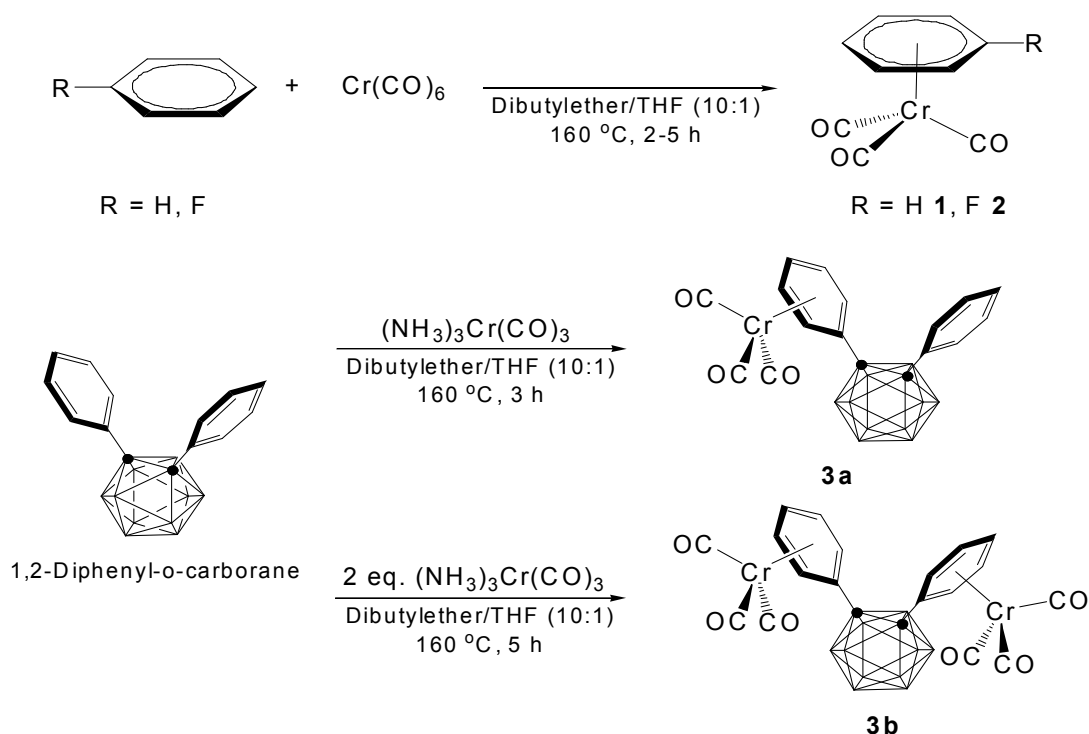
### Characterization of $\sigma$ -borane complexes

$(\eta^6\text{-C}_6\text{H}_6)\text{Cr}(\text{CO})_2(\eta^1\text{-HBH}_2\text{-NMe}_3)$  (**4**):  $^1\text{H}$  NMR (400 MHz, 293 K, toluene- $d_8$ ):  $\delta$  -5.20 (br q, 3 H,  $J_{\text{B-H}} = 89$  Hz, B-H), 4.45 (s, 6H,  $\text{C}_6\text{H}_6$ ).  $^{11}\text{B}$  NMR (128 MHz, 223 K, toluene- $d_8$ ):  $\delta$  -15.1 (br).  $^{13}\text{C}$  NMR (100 MHz, 243 K, toluene- $d_8$ ):  $\delta$  52.4 (s,  $\text{NMe}_3$ ), 88.6 (s,  $\text{C}_6\text{H}_6$ ), 246.7 (s, CO).

## 3. Results and Discussion

### Synthesis of $\sigma$ -carboranyl chromium complexes

The reaction of the diphenyl- $\sigma$ -carborane ligand with 1 or 2 equiv. of triammoniumchromium tricarbonyl  $[(\text{NH}_3)_3\text{Cr}(\text{CO})_6]$  in di-*n*-butyl ether/THF (10:1) mixed solvent yielded  $\eta^6$ -coordinated chromium complexes of the types  $[(\eta^6\text{-diphenyl-}\sigma\text{-carborane})\text{Cr}(\text{CO})_3]$  **3a** and  $\{[\eta^6\text{-diphenyl-}\sigma\text{-carborane}][\text{Cr}(\text{CO})_3]_2\}$  **3b** in good yields (**3a**, 72 and **3b**, 64%), as shown in Scheme 1.



**Scheme 1.** Synthesis of ( $\eta^6$ -arene) $\text{Cr(CO)}_3$  complexes

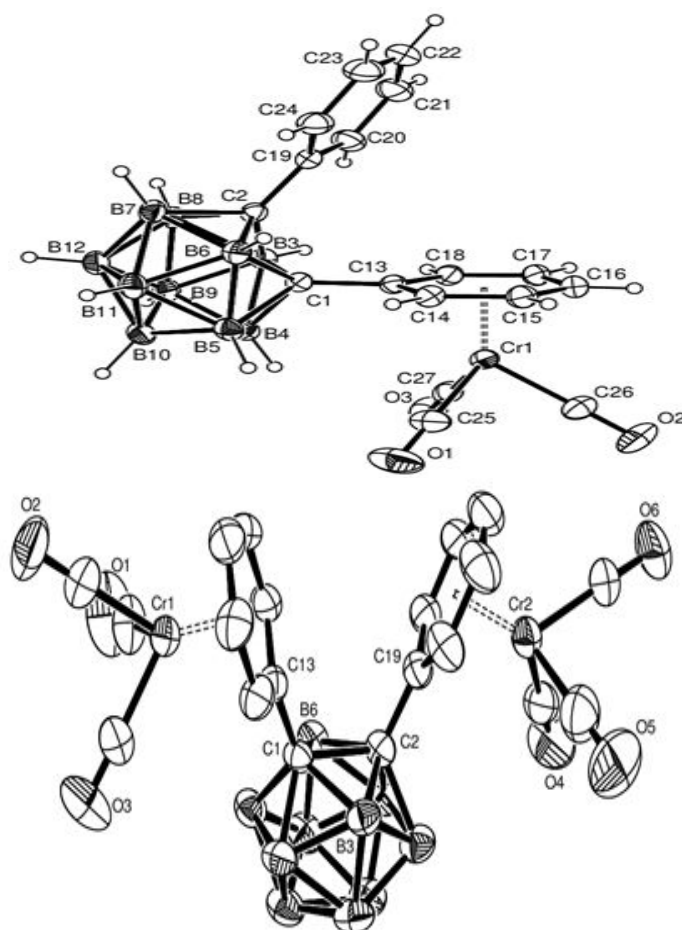
The new  $\eta^6$ -arene chromium complex (**3a**) were characterized by X-ray diffraction studies, FT-NMR ( $^1\text{H}$ ,  $^{11}\text{B}$ , and  $^{13}\text{C}$ ), and FT-IR. The spectral data for mono- (**3a**) and di-chromium complex (**3b**) suggested several structural features. The coordinated phenyl ring of diphenyl-o-carborane ligand was evident from the up-field shift of the hydrogens of the phenyl unit. The structure of compound **3a** was determined by X-ray structural analysis. X-ray data and selected interatomic distances and torsion angles are presented in Table 1 and 2. Single-crystal X-ray analysis revealed that chromium compounds **3a** and **3b** were crystallized from dichloromethane as yellow

crystals and crystallizes in the monoclinic space group  $P2_1/n$ . The asymmetric unit (Figures 1 and 2) of **3a** and **3b** comprises a single molecule that exhibits the classic ‘piano-stool’ structure, with the  $\text{Cr}(\text{CO})_3$  tripod adopting a anti-eclipsed conformation relative to the phenyl ring. This conformation is typical of the presence of an electron-acceptor substituent.<sup>28</sup> A fully eclipsed geometry is the preferred structure for substituted ( $\eta^6$ -arene) $\text{Cr}(\text{CO})_3$  molecules, with the *syn*-eclipsed conformation being adopted for electron-donating functional groups and the *anti*-eclipsed conformation being favored for electron-withdrawing groups.<sup>29</sup> The electron-acceptor character of carborane is manifest in a relative short [1.702 **3a**, 1.705 and 1.706 Å **3b**]  $\text{Cr}\cdots\text{C}_g$  distance ( $\text{C}_g$  is the ring centroid), which is characteristic of an electron-poor complex which is confirmed by high carbonyl stretching frequencies ( $\nu_{\text{max}} = 1967$  and  $1882\text{ cm}^{-1}$ ), similar to those reported previously.<sup>30</sup> The metal-centroid distance agrees with that of 1.7 Å reported for  $[\text{Cr}(\eta^6\text{-C}_6\text{H}_5\text{Cl})(\text{CO})_2\text{PPh}_3]$ <sup>31</sup> and 1.680 (5) Å observed in the fully substituted  $[\text{Cr}(\eta^6\text{-C}_6\text{Cl}_6)(\text{CO})_3]$ .<sup>30</sup> Most of the  $\text{Cr}(\text{CO})_3$  compounds with the Cr atom coordinating in a  $\eta^6$ -arene fashion, which the average Cr-C(Ph) and Cr-CO distances were 2.23 (4) and 1.83(2) Å, respectively.<sup>32</sup> Similar parameters for tricarbonylchromium with a monosubstituted  $\eta^6$ -coordinated phenyl ring are 2.22(2) and 1.84(1) Å, respectively.<sup>32</sup> These parameters are in excellent agreement with the data observed in the solid-state structure on **3a**, with are 2.21 and 1.86(2) Å, respectively, and the C13-Cr bond length [2.226(1) Å] is the longest, as expected due to the electron-withdrawing nature of the carboranyl substituent. The average C-O bond distances in carbonyl substituent are 1.142(2) Å. The C-C distances in the ligated ring of the solid-state structure of **2** [1.410(2) Å] are, as expected, longer than those of another phenyl ring [1.383(3) Å].

The crystal structures of **3a** and **3b** show that the six carbon atoms of the coordinated ring are nearly coplanar, with only very slight out-of-plane distortions. For example, the dihedral angle between the planes defined by atoms C14-C15-C17-C18 and atoms C14-C13-C18 is  $1.90(12)^\circ$ , and the torsion angles C1-C13-C14-C15 and C1-C13-C18-C17 are  $-178.09(12)^\circ$  and  $177.65(13)^\circ$ , respectively. The dihedral angle between the planes of the phenyl rings in **3a** is  $60.67(6)^\circ$ . The carbonyl groups lie between eclipsed orientations with respect to the carbon atoms of the coordinated ring. The plane formed by the three oxygen atoms is parallel to the plane of the coordinated ring [ $0.47(8)$ ]; however, the chromium atom is not symmetrically linked to the six atoms of the aromatic ring, as occurs, for example, in  $[\{C_6(CH_3)_6\}Cr(CO)_3]^{33}$  and the Cr-C<sub>g</sub>-C13 and Cr-C<sub>g</sub>-C16 angles of  $90.16^\circ$  and  $89.82^\circ$ , respectively.

**Figure 1.** ORTEP drawing (30% probability for thermal ellipsoids) of **3a**.

**Figure 2.** ORTEP drawing (30% probability for thermal ellipsoids) of **3b**

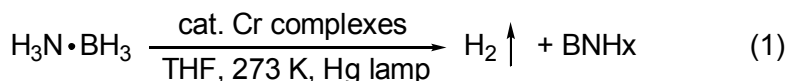


(the hydrogen atoms are omitted for clarity).

### Activation of B-H $\sigma$ -bond

Photolysis of a reaction mixture containing 1:1 stoichiometric amounts of  $\{[n$

<sup>6</sup>-diphenyl-o-carborane)][Cr(CO)<sub>3</sub>]<sub>2</sub>} (**3b**) and ammonia-borane (H<sub>3</sub>N-BH<sub>3</sub>, AB) resulted in H<sub>2</sub> evolution with the chromium complex largely remaining unreacted. The same reaction carried out using catalytic amounts of **3b** gave the same result (Eq. 1).



We noted evolution of 2.5 equiv of H<sub>2</sub> in 1.5 h when 2 mol% of (η<sup>6</sup>-o-carborane)[Cr(CO)<sub>3</sub>]<sub>2</sub> (**3b**) was used. This suggests that **3b** is an efficient catalyst for the dehydrogenation of AB (Figure 3) under photolytic conditions. These reactions result in precipitation of a white insoluble solid which is a (BNH)<sub>x</sub> type of polymer as evidenced by its IR spectrum recorded after washing several times with THF.

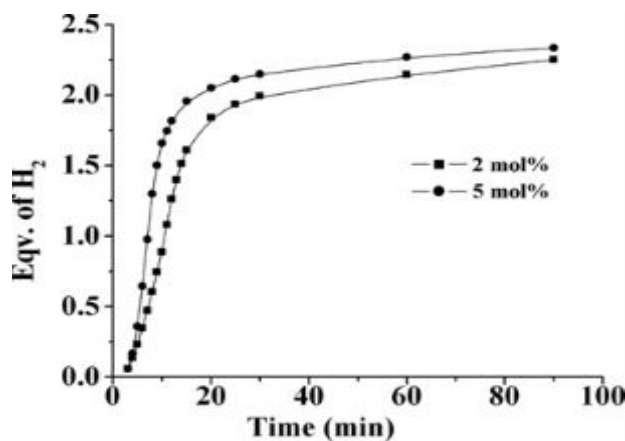
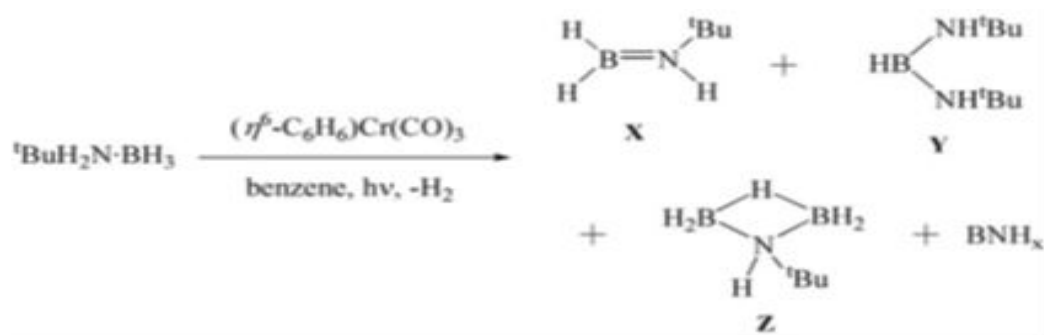


**Figure 3.** H<sub>2</sub> evolution profile of the reaction between **3b** and ammonia-borane.

When substituted amine-borane such as *tert*-butylamine borane (<sup>t</sup>BuH<sub>2</sub>N-BH<sub>3</sub>, TBAB) was used as a substrate, dehydrogenation (Scheme 2) was found to be

slower than that of ammonia-borane ( $\text{H}_3\text{N}-\text{BH}_3$ , AB). A similar B-H bond activation takes place in this case also. Here along with  $\text{H}_2\text{B}=\text{NH}^t\text{Bu}$  (**X**),  $t\text{BuNHB(H)NH}^t\text{Bu}$  (**Y**) and a  $\mu$ -hydrido species (**Z**)<sup>34</sup> were also found to be formed in the early stages of the reaction, whereas  $\text{BNH}_x$  polymer was found to be the main product of the reaction. The evolved  $\text{H}_2$  gas was collected and its volume was measured using a gas burette. In order to confirm that the evolved gas was indeed  $\text{H}_2$ , we purged it through benzene and its  $^1\text{H}$  NMR spectrum showed a singlet at  $\delta$  4.65 ppm.

The chromium complex was found to possess the amine-borane ligand based on NMR spectroscopic studies (see below). With a view to obtain a relatively stable amine-borane complex, we explored the reaction of  $(\eta^6\text{-arene})\text{Cr}(\text{CO})_3$  with trimethylamine-borane ( $\text{Me}_3\text{N}-\text{BH}_3$ ).

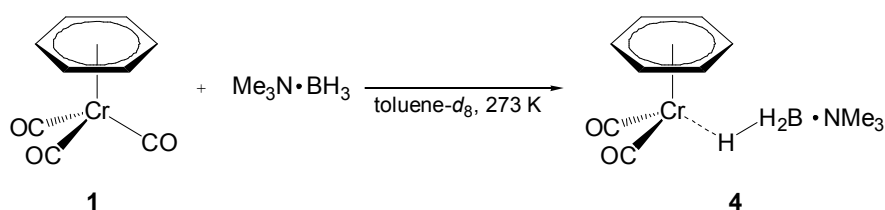


**Scheme 2.** Photolysis of chromium catalysts in presence of  $t\text{BuH}_2\text{N}-\text{BH}_3$  (TBAB).

### Observation of a $\sigma$ -borane complex



Formation of a  $\sigma$ -borane complex was noted when a toluene- $d_8$  solution of ( $\eta^6$ -arene)Cr(CO)<sub>3</sub> and Me<sub>3</sub>N-BH<sub>3</sub> (1:3 M ratio) was photolyzed at 273 K in a pressure stable NMR tube under vacuum (Scheme 3). After 1 h of photolysis, the yellow colored solution turns dark black. CO gas produced was removed by degassing the solution by freeze-pump-thaw technique and subsequently the NMR spectra of the solution were recorded at 293 K.



**Scheme 3.** Formation of a  $\sigma$ -borane complex.

The <sup>1</sup>H NMR spectrum of the reaction mixture showed the presence of  $\sigma$ -borane complex **4** with some free benzene ring. The high field region of the <sup>1</sup>H NMR spectrum of the three reaction mixtures showed two broad quartet signals corresponding to the  $\sigma$ -borane complexes. The broad quartet signal near  $\delta$  -5.0 ppm is assigned to the B-H hydrogen atoms of the benzene ring containing  $\sigma$ -borane complex ( $\eta^6$ -C<sub>6</sub>H<sub>6</sub>)Cr(CO)<sub>2</sub>( $\eta^1$ -HBH<sub>2</sub>-NMe<sub>3</sub>). Both of the signals in each case became sharp singlets upon boron decoupling (Figure 4a). The <sup>11</sup>B NMR spectrum, on the other hand showed a broad peak around  $\delta$  -15.0 ppm together with a signal for a large amount of the unreacted starting material (Me<sub>3</sub>N-BH<sub>3</sub>) (quartet). Upon <sup>1</sup>H decoupling, the <sup>11</sup>B NMR spectrum showed two singlets for the  $\sigma$ -borane complex and the unreacted starting material (Figure 4b).

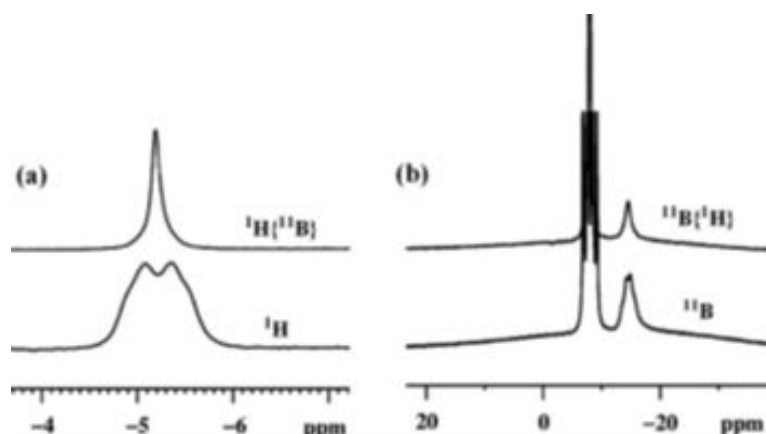


**Figure 4.** (a) Partial  $^1\text{H}$  (bottom) and  $^1\text{H}\{^{11}\text{B}\}$  (top) NMR spectra (toluene- $d_8$ , 293 K) of the high field region, and (b)  $^{11}\text{B}$  (bottom) and  $^{11}\text{B}\{^1\text{H}\}$  (top) NMR spectra (toluene- $d_8$ , 273 K) of the reaction mixture of **1** and  $\text{Me}_3\text{N}\cdot\text{BH}_3$  after 1 h of photolysis.

### Relative stability of the $\sigma$ -borane complexes

Almost all the  $\sigma$ -borane complexes reported to date have been found to be fairly unstable at ambient conditions because of the weak M-H-B interaction. Either they were observed transiently or characterized in solution. Our efforts to isolate **4** at low temperature were unsuccessful due to its extremely unstable nature. Upon standing for about 48 h at 273 K, decomposition of the  $\sigma$ -borane complex **4** take place to afford the free arene in solution and an insoluble green-colored precipitate which could not be characterized further. However, acquiring NMR data of the  $\sigma$ -borane

complexes at 293 K were successful immediately after warming the solution up to that temperature.

In complexes wherein a  $\sigma$ -bond of the ligand is bound to the metal, e.g., dihydrogen or silane complexes, in addition to sigma donation of electron density from the  $\sigma$ -bonded species, some amount of back donation from the metal to the antibonding molecular orbitals of the sigma bonded moiety is necessary for the interaction to be stable. In the case of dihydrogen complexes with  $M-(\eta^2-H_2)$  interaction, the  $\sigma$ -orbital of dihydrogen donates electron density to the metal and its  $\sigma^*$ -orbital accepts electron density from the metal via back donation. This results in a fairly stable H-H interaction with the metal; the H-H bond however, gets weakened upon binding to the metal.

It is a well established 3c-2e bond.  $M-(B-H)$  is also a 3c-2e bond. Presence of electron withdrawing group on the  $\eta^6$ -arene ligand offers better stability for the  $\sigma$ -borane complexes. However,  $(\eta^6\text{-arene})Cr(CO)_3$  loses the arene moiety during photolysis if the arene ring is electron deficient. The  $\sigma$ -borane complex **4** has one CO ligand trans to the borane ligand. Therefore, stabilization of Cr-borane interaction is brought about by the  $\pi$ -acceptance of that CO ligand. In our arene containing piano-stool structured  $\sigma$ -borane complex, this arrangement is not present; this is the reason for its limited stability in comparison to the stability of **4**. Therefore, a suitable balance between these two is required to obtain an arene containing  $\sigma$ -borane complex in reasonable yield. The  $\nu(CO)$  gives an indication of the electronic features of the arene metal tricarbonyl complex. The sharper, greater energy IR band (A band) of  $C=O$  in **4** is the highest, which suggests that the metal center is the more electron deficient than the starting material. The

thermodynamic stability of the  $\sigma$ -borane complex is governed by the strength of the M-H-B interaction which is solely dependent on the  $\sigma$ -donation from borane.<sup>14</sup> Since boranes are very weak  $\sigma$ -donor ligands, an electron deficient metal center is required to have a stable M-H-B 3c-2e bond. More electrophilic the metal center is, more  $\sigma$ -donation from the borane ligand and more stable the  $\sigma$ -borane complex. Here, **4** which possesses the most electrophilic Cr(0) center resulted in the most stable  $\sigma$ -borane complex among the three. However, for dihydrogen complexes recently reported by Heinekey and co-workers, ( $\eta^6$ -arene)Cr(CO)<sub>2</sub>(H<sub>2</sub>), the stability follows the reverse order, because the strength of metal-H<sub>2</sub> interaction also accounts for M to L back-bonding, which could be increased by introducing electron donating group on the arene ring.<sup>16</sup>

LUMO energy stabilization is clearly seen from Ph<sub>2</sub>C<sub>2</sub> and **3a** to **3b**. Previously, the HOMO-LUMO gap of 5.78 eV of Ph<sub>2</sub>C<sub>2</sub> was reported by measuring the UV-Vis spectra. As shown in Figure 5 and 6, DFT/TDDFT calculations were performed on the **3a** and **3b**, and the geometries and geometrical parameters correspond well to the X-ray crystallographic structures. In comparison to diphenyl-o-carborane, the optimized geometry for chromium complexes **3a** and **3b** reveals that the compositions of the LUMO frontier orbitals are similar to those found in the optimized geometry for diphenyl-o-carborane and the small HOMO-LUMO gap (4.05 **3a** and 3.87 **3b** eV, respectively) accounts in part for the stability of this compound. The LUMO is associated with the two C-substituted phenyl rings and partially carborane and chromium metal atoms.

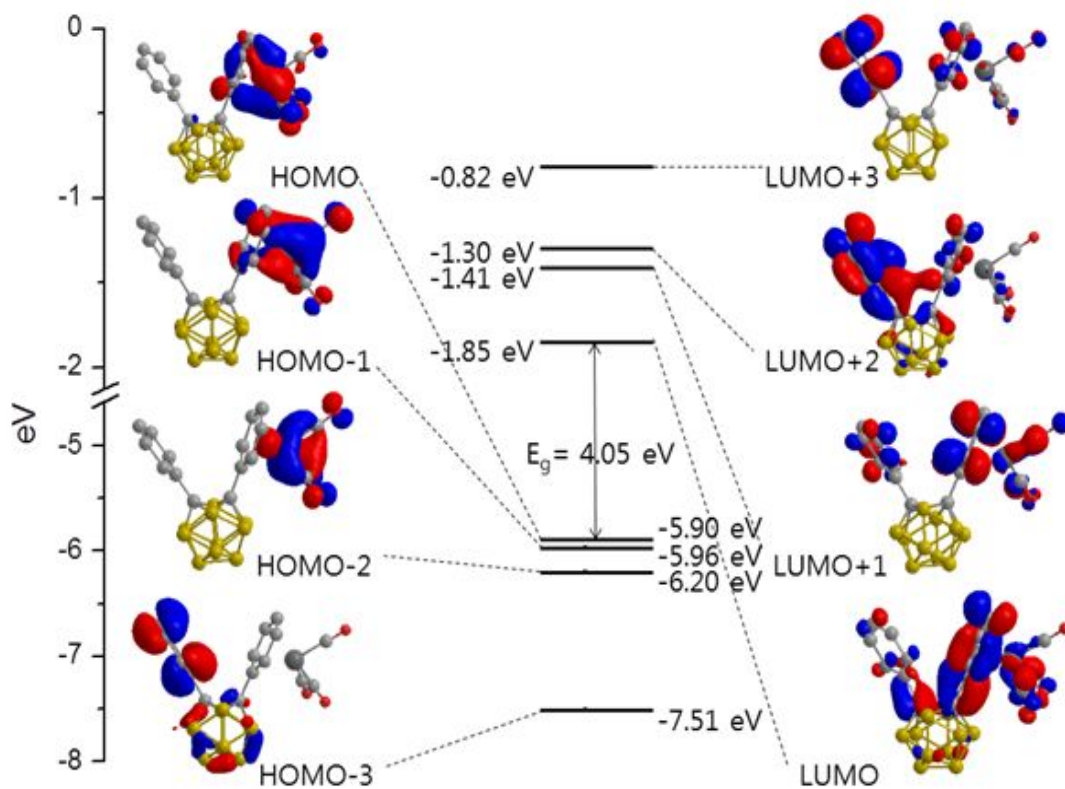


**Figure 5.** Energy levels and isodensity plots (isodensity contour = 0.03 a.u.) for selected occupied and unoccupied molecular orbitals of **3a** obtained by DFT

calculations.

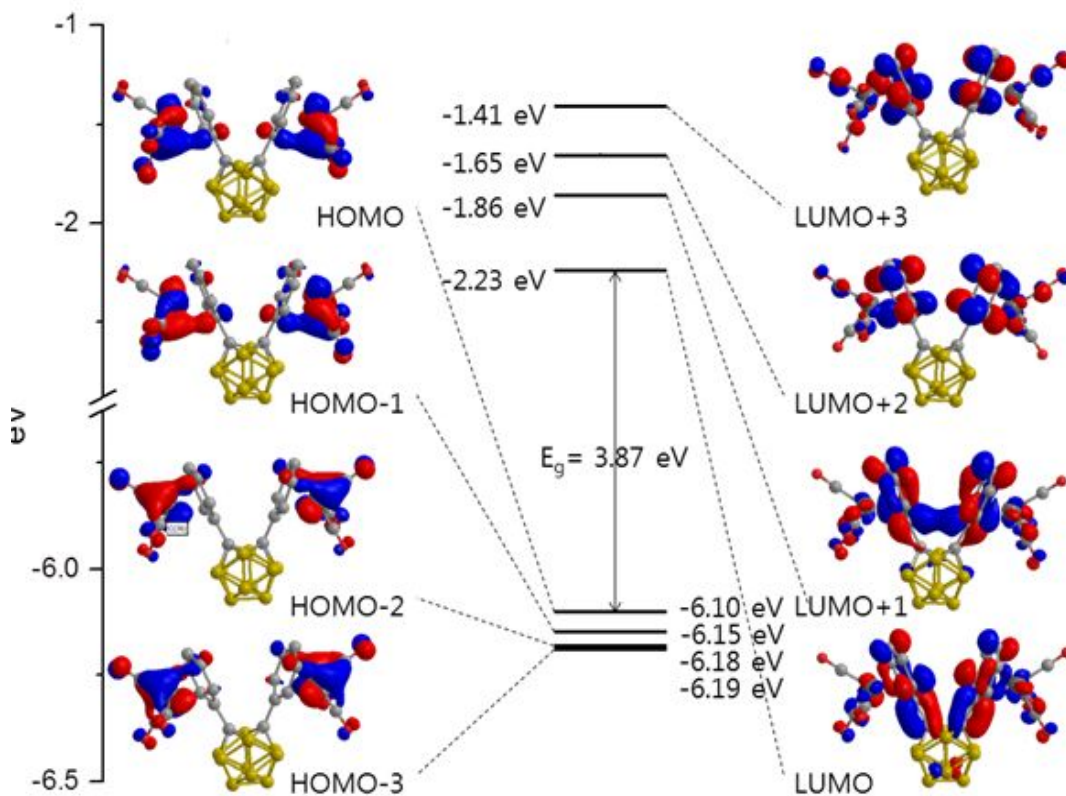


**Figure 6.** Energy levels and isodensity plots (isodensity contour = 0.03 a.u.) for selected occupied and unoccupied molecular orbitals of **3b** obtained by DFT calculations

To evaluate the  $(\eta^6\text{-arene})\text{Cr}(\text{CO})_3$  catalysts taking part in the activation of AB dehydrogenation, as shown in Figure 7, the dehydrogenation of the AB semi-solid

fuels in Cr catalysts was performed to compare the kinetic profiles. A 20 min measurement time maximized the all ( $\eta^6$ -arene)Cr(CO)<sub>3</sub> catalysts. Without o-carborane unit, AB/catalyst dehydrogenations was sluggish even at 80 °C, only producing 0.28 and 0.53 equivalents of H<sub>2</sub> in 20 min for **1** and **2**, respectively, and the reaction was completed with a total H<sub>2</sub> amount of 1.17 equivalents in 120 min. However, the participation of o-carborane was noticeable during the dehydrogenation kinetics for **3a** during the initial 20 min time span, 1.3 equivalents of H<sub>2</sub> was released; 1.7 equivalents of H<sub>2</sub> was released in 60 min, and finally it subsided with 1.8 equivalents of H<sub>2</sub> in 250 min. The optimal H<sub>2</sub> liberation was accomplished for **3a** and **3b** with o-carborane unit by releasing 2.0 and 2.3 equivalents of H<sub>2</sub> in 20 and 60 min time intervals, respectively; this finally subsided with a release of 2.4 equivalents of H<sub>2</sub> in 250 min.

From these experiments, it is evident that mixing the o-carboranyl chromium catalysts and AB system significantly increased the AB dehydrogenation kinetics for the AB/solvent semi-solid fuels, regardless of the fuel ratios at temperatures of <100 °C

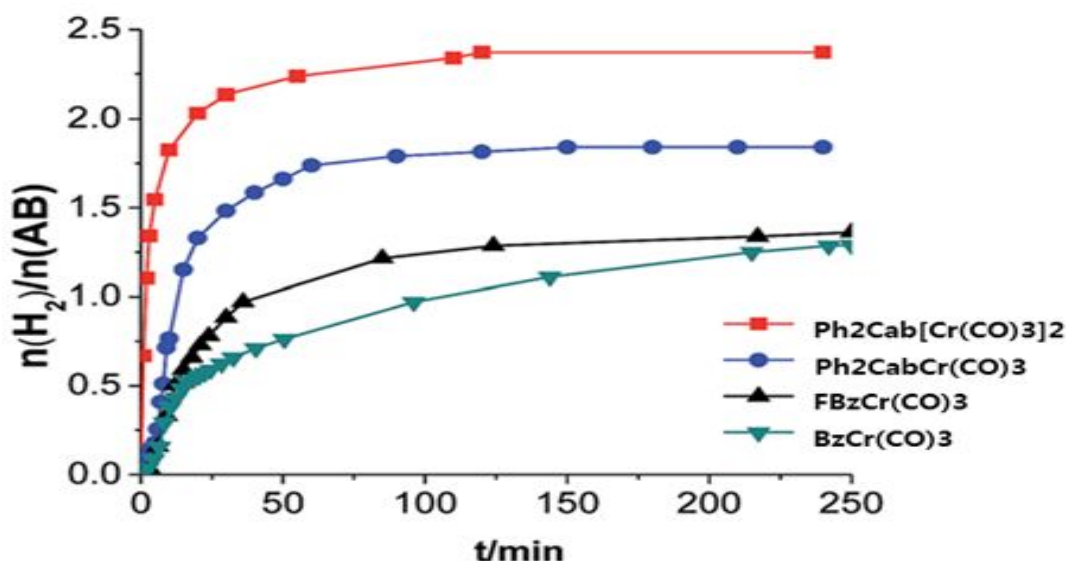


**Figure 7.** AB dehydrogenation kinetic profiles for ( $\eta^6$ -arene) $\text{Cr}(\text{CO})_3$  catalysts **1**, **2**, **3a**, and **3b**.

Kinetic isotope effect (KIE) values of 2.5, 8.2, and 9.5 were measured for  $\text{ND}_3\text{BH}_3$ ,  $\text{NH}_3\text{BD}_3$ , and  $\text{ND}_3\text{BD}_3$ , respectively, indicating that the B-H and B-D bonds weakened considerably (Figure 8). To further consolidate the facile B-H activation, a series of alkyl and aryl ABs was examined in order to show that the  $\text{H}_2$  release amount was dependent on the number of hydrogen atoms at the boron atom and that the reaction kinetics slowed in accordance with the bulkiness of the substituents at both the boron and nitrogen atoms. Most of the AB and *N*-alkyl and -aryl AB samples discharged 2.0 equiv of  $\text{H}_2$  in < 60 s, whereas *B*-alkyl and -aryl ABs released only 1 equiv  $\text{H}_2$  after 90 s. Again, B-H activation<sup>35</sup> dictated the rate of AB dehydrogenation kinetics and produced only 1.5 equiv of  $\text{H}_2$  over an extended period (1500 s).



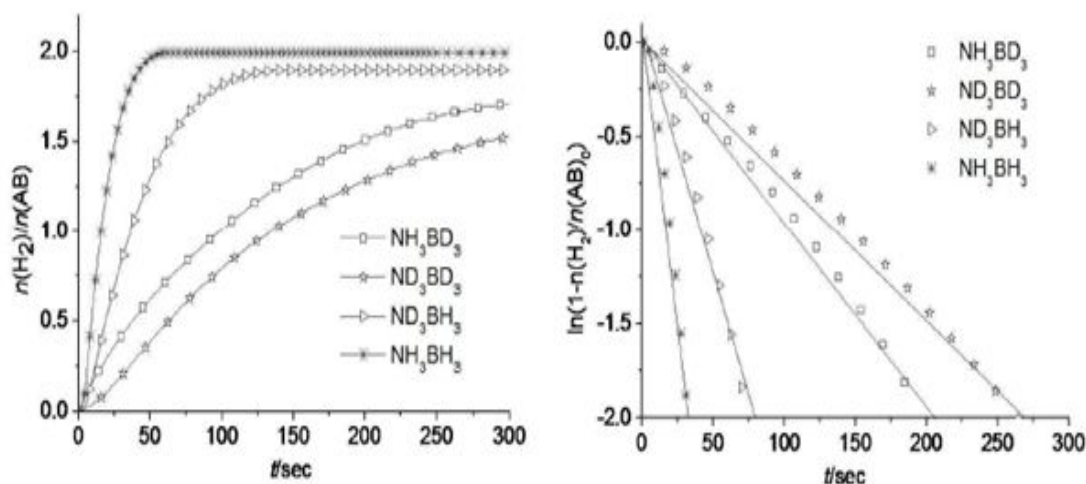


**Figure 8.** (a) Dehydrogenation kinetic isotope effect (KIE) plots for AB and deuterated ABs with catalyst **3b** at 25 °C and (b) their corresponding logarithmic plots. The straight lines in (b) were obtained from linear regression analysis of the data points.

## 4. Conclusion

Sigma borane complexes of the type ( $\eta^6$ -arene)Cr(CO)<sub>2</sub> ( $\eta^1$ -HBH<sub>2</sub>-NMe<sub>3</sub>) could be prepared via photolysis of ( $\eta^6$ -arene)Cr(CO)<sub>3</sub> and Me<sub>3</sub>N-BH<sub>3</sub>. These derivatives are unstable towards decomposition. They could be characterized in solution using multinuclear NMR spectroscopy. From this study, we conclude that the presence of electrophilic metal center imparts relatively greater stability (in solution at low temperature) compared to others in this series of complexes. Work is in progress to obtain stable and isolable  $\sigma$ -borane complexes.

We have found that the LUMO of Ph<sub>2</sub>C<sub>2</sub> was stabilized through the metallation to phenyl unit(s) found in **3a** and **3b**, and **3a** and **3b** functions as a strong  $\pi$ -acceptor

to form a stable new type of organometallic complexes through the metal-to-ligand back-bonding interaction  $[\text{Cr(d)}\text{-Ph}(\pi^*)\text{-o-carboranyl C-C (}\sigma^*)]$ . This study clearly shows the electron withdrawing properties of o-carborane, provided that two phenyl groups are juxtaposed and paralleled.

When  $(\eta^6\text{-arene})\text{Cr(CO)}_3$  catalysts based on o-carborane were applied for the generation of  $\text{H}_2$  from AB/solventsemi-solid state system, a high hydrogen storage system (19.5 st%) was obtained with the optimal performance of AB dehydrogenation.

## 5. References

1. Lata, C. J. Crudden, C. M. *J. Am. Chem. Soc.* **2010**, 132, 131.
2. Hebden, T. J. Denney, M. C. Pons, V. Piccoli, P. M. B. Koetzle, T. F. Schultz, A. J. Kaminsky, W. Goldberg, K. I. Heinekey, D. M. *J. Am. Chem. Soc.* **2008**, 130, 10812.
3. Smythe, N. C. Gordon, J. C. *Eur. J. Inorg. Chem.* **2010**, 509.
4. Bernskoetter, W. H. Schauer, C. K. Goldberg, K. I. Brookhart, M. *Science* **2009**, 326, 553.

5. Snow, S. A. Shimoi, M. Ostler, C. D. Thompson, B. K. Kodama, C. Parry, R. W. *Inorg. Chem.* **1984**, 23, 512.
6. Kubas, G. J. *Chem. Rev.* **2007**, 107, 4152.
7. Lin, Z. *Struct. Bonding* **2008**, 130, 123.
8. Pandey, K. K. *Coord. Chem. Rev.* **2009**, 253, 37.
9. Alcaraz, G. Grellier, M. Sabo-Etienne, S. *Acc. Chem. Res.* **2009**, 42, 1640.
10. Alcaraz, G. Sabo-Etienne, S. *Angew. Chem., Int. Ed.* **2010**, 49, 7170.
11. Kakizawa, T. Kawano, Y. Shimoi, M. *Organometallics* **2001**, 20, 3211.
12. Shimoi, M. Nagai, S.-I. Ichikawa, M. Kawano, Y. Katoh, K. Uruichi, M. Ogino, H. *J. Am. Chem. Soc.* **1999**, 121, 11704.
13. Kawano, Y. Uruichi, M. Shimoi, M. Taki, S. Kawaguchi, T. Kakizawa, T. Ogino, H. *J. Am. Chem. Soc.* **2009**, 131, 14946.
14. Kawano, Y. Yamaguchi, K. Miyake, S.-Y. Kakizawa, T. Shimoi, M. *Chem. Eur. J.* **2007**, 13, 6920.
15. Kawano, Y. Hashiva, M. Shimoi, M. *Organometallics* **2006**, 25, 4420.
16. Egbert, J. D. Heinekey, D. M. *Organometallics* **2010**, 29, 3387.
17. Jetz, W. Graham, W. A. G. *Inorg. Chem.* **1971**, 10, 4.
18. Glavee, G. N. Jagirdar, B. R. Schneider, J. J. Klabunde, K. J. Radonovich,

- L. J. Dodd, K. *Organometallics* **1992**, *11*, 1043.
19. Ramachandran, P. V. Gagare, P. D. *Inorg. Chem.* **2007**, *46*, 7810.
20. Mahaffy, C. A. L. Pauson, P. L. *Inorg. Synth.* **1979**, *19*, 154.
21. Jin, G. F.; Hwang, J. -H.; Lee, J. -D.; Wee, K. -R.; Suh, I. -H.; Kang, S. O. *Chem. Commun.* **2013**, *49*, 9398.
22. *SMART and SAINT* Bruker Analytical X-Ray Division: Madison,WI, 2002.
23. Sheldrick, G. M. *SHELXTL-PLUS Software Package* Bruker Analytical X-Ray Division: Madison, WI, 2002.
24. (a) Lee, C.; Yang, W.; Parr, R. G. *Phys. Rev. B* **1988**, *37*, 785. (b) Vosko, S. H. Wilk, L. Nusair, M. *Can. J. Phys.* **1980**, *58*, 1200. (c) Becke, A.D. *J. Chem. Phys.* **1993**, *98*, 5648. (d) Stephens, P. J. Devlin, F. J. Chabalowski, C. F. Frisch, M. J. *J. Phys. Chem.* **1994**, *98*, 11623.
25. Hay, P. J.; Wadt, W. R. *J. Chem. Phys.* **1985**, *82*, 299.
26. (a) "Gaussian Basis Sets for Molecular Calculations" S.Huzinaga, J.Andzelm, M.Klobukowski, E.Radzio-Andzelm, Y.Sakai, H.Tatewaki Elsevier, Amsterdam, 1984. (b) Davidson, E. R. Feller, D. *Chem. Rev.* **1986**, *86*, 681.
27. Frisch, M. J.; Trucks, G.W.; Schlegel, H. B.; Scuseria, G. E.; Robb, M. A.; Cheeseman, J. R.; Scalmani, G.; Barone, V.; Mennucci, B.; Petersson, G. A.; Nakatsuji, H.; Caricato, M.; Li, X.; Hratchian, H. P.; Izmaylov, A. F.; Bloino, J.; Zheng, G.; Sonnenberg, J. L.; Hada, M.; Ehara, M.; Toyota, K.; Fukuda, R.;

Hasegawa, J.; Ishida, M.; Nakajima, T.; Honda, Y.; Kitao, O.; Nakai, H.; Vreven, T.; Montgomery Jr., J. A.; Peralta, J. E.; Ogliaro, F.; Bearpark, M.; Heyd, J. J.; Brothers, E.; Kudin, K. N.; Staroverov, V. N.; Keith, T.; Kobayashi, R.; Normand, J.; Raghavachari, K.; Rendell, A.; Burant, J. C.; Iyengar, S. S.; Tomasi, J.; Cossi, M.; Rega, N.; Millam, J. M.; Klene, M.; Knox, J. E.; Cross, J. B.; Bakken, V.; Adamo, C.; Jaramillo, J.; Gomperts, R.; Stratmann, R. E.; Yazyev, O.; Austin, A. J.; Cammi, R.; Pomelli, C.; Ochterski, J. W.; Martin, R. L.; Morokuma, K.; Zakrzewski, V. G.; Voth, G. A.; Salvador, P.; Dannenberg, J. J.; Dapprich, S.; Daniels, A. D.; Farkas, O.; Foresman, J. B.; Ortiz, J. V.; Cioslowski, J.; Fox, D. J., Gaussian 09, Revision B.01, Gaussian, Inc., Wallingford CT, 2010.

28. Muetterties, E. L.; Bleeke, J. R.; Wucherer, E. J.; Albright, T. A. *Chem. Rev.* **1982**, 82, 499.

29. Besançon, J.; Tirouflet, J.; Card, A.; Dusauroy, Y. *J. Organomet. Chem.* **1973**, 59, 267.

30. Gassman, P. G.; Deck, P. A. *Organometallics* **1994**, 13, 1934.

31. Eglin, J. L.; Smith, L. T. *Inorg. Chim. Acta* **2001**, 320, 198.

32. Czerwinski, C. J. Guzei, I. A. Cordes, T. J. Czerwinski, K. M. Mlodik, N. A. *Acta Cryst.* **2003**, C59, m499.

33. Byers, B. P.; Hall, M. B. *Inorg. Chem.* **1987**, 26, 2186.

34. Schwartz, I. D.; Keller, P. C. *J. Am. Chem. Soc.* **1972**, 94, 3015.

35. Rossin, A.; Caporali, M.; Gonsalvi, L.; Guerri, A.; Lledós, A.; Peruzzini, M.; Zanobini, F. *Eur. J. Inorg. Chem.* **2009**, 3055.

**Table 1.** Crystal data and structure refinement

	<b>3a</b>	<b>3b</b>
Empirical formula	C <sub>17</sub> H <sub>20</sub> B <sub>10</sub> CrO <sub>3</sub>	C <sub>20</sub> H <sub>23</sub> B <sub>10</sub> Cr <sub>2</sub> O <sub>6</sub>
Formula weight	432.45	571.50
Temperature	293(2) K	293(2) K
Wavelength	0.71073 Å	0.71073 Å
Crystal system,	Monoclinic,	Monoclinic,
space group	<i>P</i> 2 <sub>1</sub> /n	<i>P</i> 2 <sub>1</sub> /n
Unit cell dimensions	<i>a</i> = 8.2745(7) Å	<i>a</i> = 12.5359(8) Å
	<i>b</i> = 15.5626(13) Å	<i>b</i> = 12.9150(8) Å
	<i>c</i> = 16.2094(14) Å	<i>c</i> = 13.3882(8) Å
Volume	2087.3(3) Å <sup>3</sup>	2137.1(2) Å <sup>3</sup>
Z, D <sub>calc</sub>	4, 1.185 g/cm <sup>3</sup>	4, 1.158 g/cm <sup>3</sup>
<i>F</i> (000)	776	776
Crystal size	0.10 × 0.08 × 0.05 mm	0.40 × 0.20 × 0.20 mm
Θ range for data collection	1.81 to 28.34°	2.06 to 28.36°
Limiting indices	-11 ≤ <i>h</i> ≤ 10, -20 ≤ <i>k</i> ≤ 20, -21 ≤ <i>l</i> ≤ 21	-16 ≤ <i>h</i> ≤ 16, -17 ≤ <i>k</i> ≤ 17, -17 ≤ <i>l</i> ≤ 17
Reflections collected / unique	21438 / 5180 [ <i>R</i> (int) = 0.0326]	28537 / 5335 [ <i>R</i> (int) = 0.0335]
Completeness to Θ = 25.96	99.9 %	99.8 %

Refinement method	Full-matrix least-squares on $F^2$	Full-matrix least-squares on $F^2$
Data / restraints / parameters	5180 / 0 / 271	5335 / 0 / 280
Goodness-of-fit on $F^2$	1.019	1.054
Final R indices [ $I > 2\sigma(I)$ ]	$^aR_1 = 0.0427$ , $^b wR_2 = 0.1155$	$^aR_1 = 0.0592$ , $^b wR_2 = 0.1565$
R indices (all data)	$^aR_1 = 0.0458$ , $^b wR_2 = 0.1190$	$^aR_1 = 0.0770$ , $^b wR_2 = 0.1759$
Largest diff. peak and hole	0.263 and $-0.191 \text{ e.}\text{\AA}^{-3}$	0.270 and $-0.305 \text{ e.}\text{\AA}^{-3}$

**Table 2.** Selected bond lengths [ $\text{\AA}$ ] and torsion angles [ $^\circ$ ] for **3a** and **3b**

Bond lengths [Å]			Torsion angles [°]	
3a	C(1)-C(13)	1.499	C13-C18 vs C19-C24	88.73(6)
	C(1)-C(2)	1.741		
	C(2)-C(19)	1.500		
	C <sub>cent</sub> -Cr	1.702		
3b	C(1)-C(13)	1.507	C13-C18 vs C19-C24	49.12(7)
	C(1)-C(2)	1.725		
	C(2)-C(19)	1.506		
	C <sub>cent</sub> -Cr(1)	1.705		
	C <sub>cent</sub> -Cr(2)	1.706		



